Inkjet Printed Electrode Arrays for Potential Modulation of DNA Self-Assembled Monolayers on Gold

ARTICLE *in* ANALYTICAL CHEMISTRY · NOVEMBER 2008

Impact Factor: 5.64 · DOI: 10.1021/ac801420h · Source: PubMed

4 AUTHORS, INCLUDING:

Yunchao Li
Beijing Normal University
41 PUBLICATIONS **1,247** CITATIONS
SEE PROFILE

Paul C H Li
Simon Fraser University
75 PUBLICATIONS **1,181** CITATIONS
SEE PROFILE

Anal. Chem. **2008,** *80,* 8814–8821

Inkjet Printed Electrode Arrays for Potential Modulation of DNA Self-Assembled Monolayers on Gold

Yunchao Li,[†,‡] Paul C. H. Li,[†] M. (Ash) Parameswaran,[§] and Hua-Zhong Yu*[,†]

Department of Chemistry and School of Engineering Science, Simon Fraser University, Burnaby, British Columbia V5A 1S6, Canada, and Department of Chemistry, Beijing Normal University, Beijing100875, China

In this paper, we report a novel and cost-effective fabrication technique to produce electrode arrays that can be used for monitoring and electrical manipulaton of the molecular orientation of DNA self-assembled monolayers (SAMs) on gold. The electrode arrays were prepared from gold coated glass sides or compact discs (CD-Rs) by using standard office inkjet printers without any hardware or software modifications. In this method, electrode arrays of varied shape and size (from submillimeter to centimeter) can be rapidly fabricated and are suitable for standard electrochemical measurements. We were able to use a dual-channel potentiostat to control the electrodes individually and a fluorescence (FL) scanner to image the electrode array simultaneously. With such an integrated modulation setup, the structural switching behavior (from "lying" to "standing" position) and the enhanced hybridization reactivity of thiolate DNA SAMs on gold under potential control have been successfully demonstrated.

The technology of DNA microarrays is proving to be one of the most powerful tools for high-throughput analysis of genome sequence, expression, and mutations. Typical biochips are based on fluorescence (FL) detection and fabricated on glass, silicon, or plastic substrates.[1−8] Recently, noble metals (particularly gold) have become promising alternatives due to their simple surface chemistry, ease of attaching DNA probes, and good electrical conductivity, which allows the possibility of electrical/electrochemical signal read-out protocols.[9−12] For example, thiol-modified DNA strands can spontaneously adsorb on gold to form robust, highly oriented self-assembled monolayers (SAMs), which can be further characterized electrochemically. One of the limitations of such systems is the incompatibility with FL detection, as the FL from the labeled target strands may be quenched upon hybridization on a gold electrode surface.[12−14]

It has been demonstrated that the above-mentioned FL quenching issue can be managed to some extent by modulating the molecular conformation of immobilized DNA probes to increase the distance between the fluorescent tags and the electrode surface. This may be accomplished by applying an interfacial electric field, which can be controlled by changing the electrode potentials. Kelley et al. first reported the significant change in DNA film thickness using in situ atomic force microcopy (AFM) by switching the potential applied to the double-stranded DNA (dsDNA) SAM-modified gold electrode.[15] By monitoring the FL intensity, Rant et al. demonstrated that the conformation of both single-stranded DNA (ssDNA) and dsDNA monolayers can be reproducibly switched between "lying" and "standing" positions by alternating the electrode potentials.[16,17] Furthermore, they were able to employ such "structural switchable" ssDNA SAMs for the label-free detection of target DNA strands, based on the difference of the switching dynamics between ssDNA and dsDNA monolayers.[18] Besides the ability to modulate the conformation of DNA SAMs, interfacial electric fields have also been shown to induce DNA stretching,[19,20] transport,[21,22] immobilization/release,[23−26] as well as on-chip hybridization.[21,23,26−29] Heller and co-workers developed an arrayed platform for DNA hybridization, for which DNA probes were immobilized on an agarose permeation layer (coated on the electrode surface) and an positive electric field served as the driving force to move and concentrate DNA target

* To whom correspondence should be addressed. E-mail: hogan_yu@sfu.ca. Fax: (778) 782-3765.

† Department of Chemistry, Simon Fraser University.

‡ Department of Chemistry, Beijing Normal University.

§ School of Engineering Science, Simon Fraser University.

(1) Pirrung, M. *Angew. Chem., Int. Ed.* **2002**, *41*, 1276–1289, and references therein.

(2) Cheung, V. G.; Morley, M.; Aguilar, F.; Massimi, A.; Kucherlapat, R.; Childs, G. *Nat. Genet.* **1999**, *21*, 15–19, and references therein.

(3) Zammatteo, N.; Jeanmart, L.; Hamels, S.; Courtois, S.; Louette, P.; Hevesi, L.; Remacle, J. *Anal. Biochem.* **2000**, *280*, 143–150.

(4) Rogers, Y. H.; Jiang-Baucom, P.; Huang, Z. J.; Bogdanov, V.; Anderson, S.; Boyce-Jacino, M. T. *Anal. Biochem.* **1999**, *266*, 23–30.

(5) Lenigk, R.; Carles, M.; Ip, N. Y.; Suher, N. J. *Langmuir* **2001**, *17*, 2497–2501.

(6) Oh, S. J.; Cho, S. J.; Kim, C. K.; Park, J. W. *Langmuir* **2002**, *18*, 1764–1769.

(7) Bertucci, F.; Loriod, B.; Nasser, V.; Granjeaud, S.; Tagett, R.; Braud, A. C.; Patrice Viens, P.; Houlgatte, R.; Birnbaum, D.; Nguyen, C. C. R. *Biologies* **2003**, *326*, 1031–1039.

(8) Li, Y.; Wang, Z.; Ou, L. M. L.; Yu, H.-Z. *Anal. Chem.* **2007**, *79*, 426–433.

(9) Herne, T. M.; Tarlov, M. J. *J. Am. Chem. Soc.* **1997**, *119*, 8916–8920.

(10) Steel, A. B.; Herne, T. M.; Tarlov, M. J. *Anal. Chem.* **1998**, *70*, 4670–4677.

(11) Park, S. J.; Taton, T. A.; Mirkin, C. A. *Science* **2002**, *295*, 1503–1506.

(12) Lee, H. J.; Goodrich, T. T.; Corn, R. M. *Anal. Chem.* **2001**, *73*, 5525–5531.

(13) Chance, R. R.; Prock, A.; Silbey, R. *Adv. Chem. Phys.* **1978**, *37*, 1–65.

(14) Barnes, W. L. *J. Mod. Opt.* **1998**, *45*, 661–699.

(15) Kelley, S. O.; Barton, J. K.; Jackson, N. M.; McPherson, L. D.; Potter, A. B.; Spain, E. M.; Allen, M. J.; Hill, M. G. *Langmuir* **1998**, *14*, 6781–6784.

(16) Rant, U.; Arinaga, K.; Fujita, S.; Yokoyama, N.; Abstreiter, G.; Tornow, M. *Nano Lett.* **2004**, *4*, 2441–2445.

(17) Rant, U.; Arinaga, K.; Fujita, S.; Yokoyama, N.; Abstreiter, G.; Tornow, M. *Org. Biomol. Chem.* **2006**, *4*, 3448–3455.

(18) Rant, U.; Arinaga, K.; Scherer, S.; Pringsheim, E.; Fujita, S.; Yokoyama, N.; Abstreiter, G.; Tornow, M.; Abstreiter, G. *Proc. Natl. Acad. Sci. U.S.A.* **2007**, *104*, 17364–17369.

10.1021/ac801420h CCC: $40.75
Published on Web 10/24/2008

strands around the selected test sites.[27] On the basis of the surface plasmon resonance (SPR) spectroscopic results,[28] Heaton et al. concluded that an applied electric field not only helps to modulate DNA hybridization rate but also improves the discrimination of base mismatches. Fixe et al. further demonstrated that the surface density of immobilized DNA strands, the hybridization rate, and the mismatch discrimination efficiency could be improved or enhanced by exerting an alternate electric field (square-wave voltage pluses) to the electrode of interest.[26,29]

Electrode arrays or microelectrode sets are ideal platforms for parallel electrochemical analysis and manipulation of multiple analytes;[30−32] however, their preparation is generally limited to well-equipped laboratories due to the requirement for expensive infrastructure. For example, the processing steps for lithography (including optical and e-beam) and microcontact printing (or soft lithography), the two most common methods for microfabrication,[27,30,31,33,34] require special radiation sources, high-resolution mask plates, and clean-room facilities. Therefore, it is of practical importance to develop low-cost and easy-access preparation methods for electrode arrays and microstructured electrodes. Daniel et al. fabricated submillimeter tailored gold electrode sets on gold CD-R via heat-transferring the laser printing toner and subsequent wet chemical etching.[35] Xu et al. took a nanoparticle (NP) site-selective deposition route to prepare patterned gold film on a plastic substrate; the deposited NPs were then treated at high temperature to obtain a good conductivity.[36] Kamyshny et al. reported another method of inkjet printing metal nanoparticle "ink" to prepare conductive patterns; the prepared patterns were sintered to reduce their electrical resistance.[37] Very recently, Cho et al. has reported that unmodified office printers can be used to prepare multiplex chemical sensors from gold CD-Rs.[38]

Table 1. Oligonucleotide Sequences of Marker, Probe, and Target DNA Strands

DNA sample	sequence
marker	HS-$(CH_2)_6$-O-5′-CTG TAT TGA GTT GTA TCG TGT GGT GTA TTT-3′-Cy5
probe	HS-$(CH_2)_6$-O-5′-CTG TAT TGA GTT GTA TCG TGT GGT GTA TTT-3′
target	Cy5−5′-AAA TAC ACC ACA CGA TAC AAC TCA ATA CAG-3′

In this paper, we report a protocol of direct inkjet printing in combination with wet-chemical etching to fabricate electrode arrays from gold CD-Rs or gold-coated glass slides. Their applications for conventional electrochemical measurements and for potential modulation of the conformation of DNA SAMs on gold will be demonstrated. The ability of selectively manipulating the molecular orientation and hybridization reactivity of DNA probe strands on chip is a unique application of combining electrode array fabrication and electrochemical in situ fluorescence imaging techniques, which has not yet been explored previously.

EXPERIMENTAL SECTION

Materials and Reagents. 1-Octadecanethiol, 1-octanol, 6-mercapto-1-hexanol (MCH), tris(2-carboxyethyl)phosphine hydrochloride (TCEP), $[Ru(NH_3)_6]Cl_3$, and tris(hydroxymethyl)-aminomethane (Tris) were purchased from Sigma-Aldrich; they were of ACS reagent grade and used without further purification. All solutions were prepared with deionized water (18.3 MΩ·cm) from a Barnstead EasyPure UV/UF water system. The DNA oligomers (sequences are listed in Table 1) were obtained from Sigma-Genosys (Oakville, ON) and were purified with HPLC. Mitsui 700 MB Gold CD-Rs were obtained in bundles locally. Gold slides (100 nm Au/5 nm Cr/glass) were purchased from the Evaporated Metal Films Co. (Ithaca, NY). Sylgard 184 silicone and its curing agent for making polydimethysiloxane (PDMS) plates were obtained from Dow Corning (Midland, MI).

Electrode Fabrication. As illustrated in Scheme 1, the fabrication of gold electrode arrays consists of three steps: inkjet printing of the thiol solutions, wet chemical etching, and the resist layer removing. Before printing, the substrates (gold CD-Rs or gold slides) were first washed with concentrated HNO_3 or "piranha" solution (H_2SO_4/H_2O_2, 3:1, heated to 90 °C), and then rinsed thoroughly with deionized water. A commercial inkjet printer (Epson Stylus Photo R200/ R300) with a continuous ink system (CF4-210, CISS Solutions Co., U.K.) was used to print 1-octadecanethiol solution (0.5∼1.5 mM in isopropanol) on gold substrates to form the resist layers with the desired features. For gold CD-Rs, they can be loaded onto the front-printing tray directly (Figure 1a), while for gold slides a special sample holder was fabricated using a blank CD (as shown in Figure 1b). A free software supplied by EPSON, Print-CD, was used to create the desired electrode pattern and also to control the printing process. After the printing step, the gold CD-R was gently immersed in an aqueous etching solution containing 0.1 M $K_2S_2O_3$/1 M KOH/

(19) Ferree, S.; Blanch, H. W. *Biophys. J.* **2003**, *85*, 2539–2546.
(20) Germishuizen, W. A.; Walti, C.; Wirtz, R.; Pepper, M.; Davies, A. G.; Middelberg, A. P. J. *Nanotechnology* **2003**, *14*, 896–902.
(21) Edman, C.; Raymond, D.; Wu, D.; Tu, E.; Sosnowski, R. G.; Butler, W. F.; Nerenberg, M.; Heller, M. J. *Nucleic Acids Res.* **1997**, *25*, 4907–4914.
(22) Syrzycka, M.; Sjoerdsma, M.; Li, P. C. H.; Parameswaran, M.; Syrzycki, M.; Koch, C. A.; Utkhede, R. S. *Anal. Chim. Acta* **2003**, *484*, 1–14.
(23) Peterson, A. W.; Heaton, R. J.; Georgiadis, R. M. *Nucleic Acids Res.* **2001**, *29*, 5163–5168.
(24) Ge, C.; Liao, J.; Yu, W.; Gu, N. *Biosens. Bioelectron.* **2003**, *18*, 53–58.
(25) Takeishi, S.; Rant, U.; Fujiwara, T.; Buchholz, K.; Usuki, T.; Arinaga, K.; Takemoto, K.; Yamaguchi, Y.; Tornow, M.; Fujita, S.; Abstreiter, G.; Yokoyama, N. *J. Chem. Phys.* **2004**, *120*, 5501–5504.
(26) Fixe, F.; Branz, H. M.; Louro, N.; Chu, V.; Prazeres, D. M. F.; Conde, J. P. *Nanotechnology* **2005**, *16*, 2061–2071.
(27) Sosnowski, R. G.; Tu, E.; Butler, W. F.; O'Connell, J. P.; Heller, M. J. *Proc. Natl. Acad. Sci. U.S.A.* **1997**, *94*, 1119–1123.
(28) Heaton, R. J.; Peterson, A. W.; Georgiadis, R. M. *Proc. Natl. Acad. Sci. U.S.A.* **2001**, *98*, 3701–3704.
(29) Fixe, F.; Chu, V.; Prazeres, D. M. F.; Conde, J. P. *Biosens. Bioelectron.* **2005**, *21*, 888–893.
(30) Xu, D.; Xu, D.; Yu, X.; Liu, Z.; He, W.; Ma, Z. *Anal. Chem.* **2005**, *77*, 5107–5113.
(31) Li, X.; Zhou, Y.; Sutherland, T. C.; Baker, B.; Lee, J. S.; Kraatz, H.-B. *Anal. Chem.* **2005**, *77*, 5766–5769.
(32) Marquette, C. A.; Lawrence, M. F.; Blum, L. J. *Anal. Chem.* **2006**, *78*, 959–964.
(33) Wilbur, J. L.; Kumar, A.; Biebuyck, H. A.; Kim, E.; Whitesides, G. M. *Nanotechnology* **1996**, *7*, 452–457.
(34) Watson, M. W. L.; Abdelgawad, M.; Ye, G.; Yonson, N.; Trottier, J.; Wheeler, A. R. *Anal. Chem.* **2006**, *78*, 7877–7885.
(35) Daniel, D.; Gutz, I. G. R. *Electrochem. Commun.* **2003**, *5*, 782–786.
(36) Xu, H.; Hong, R.; Wang, X.; Arvizo, R.; You, C.; Samanta, B.; Patra, D.; Tuominen, M. T.; Rotello, V. M. *Adv. Mater.* **2007**, *19*, 1383–1386.
(37) Kamyshny, A.; Ben-Moshe, M.; Aviezer, S.; Magdassi, S. *Macromol. Rapid Commun.* **2005**, *26*, 281–288.
(38) Cho, H.; Parameswaran, M.; Yu, H.-Z. *Sens. Actuators, B* **2007**, *123*, 749–756.

Scheme 1. Preparation of Gold Electrode Arrays[a]

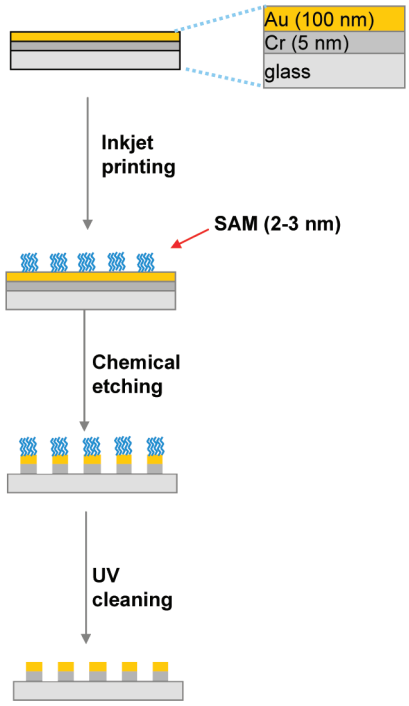

[a] (a) Inkjet printing 1-$C_{18}H_{37}SH$ "ink" on a gold substrate to form a resist layer, (b) etching the uncovered gold by immersing in a $Fe(CN)_6^{3/4-}$ + $S_2O_3^{2-}$ solution, and (c) removing the thiolate SAMs on the fabricated gold electrode surface by UV irradiation or "piranha" solution washing.

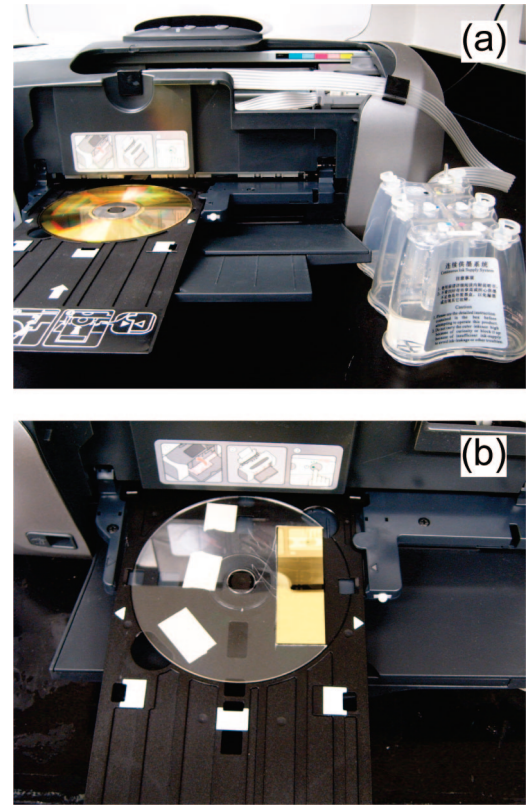

Figure 1. Optical images of the inkjet printing setup: (a) An Epson Stylus Photo R200 printer with a continuous ink system (bottom right) and (b) the CD-print tray loaded with a specially designed substrate holder for printing gold slides.

0.01 M $K_3Fe(CN)_6$/0.001 M $K_4Fe(CN)_6$ for 10~15 min.[38,39] For gold slides, we used a stronger etching solution (0.15 M $K_2S_2O_3$/1 M KOH/0.03 M $K_3Fe(CN)_6$/0.001 M $K_4Fe(CN)_6$) in 1-octanol-saturated water and a longer reaction time (40~50 min). After the etching step, the 1-octadecanethiolate SAMs on the gold surface were removed by UV exposure or washing with piranha solution.

Preparation of DNA-Modified Electrodes. To prepare thiol-terminated single-stranded DNA (HS-ssDNA) (marker or probe), the disulfide-modified oligomers were treated with 10 mM TCEP in 100 mM Tris at pH 7.4 overnight and desalted through a MicroSpin column (G-50 Sephadex). For thiol-terminated double-stranded DNA (HS-dsDNA), 10 μM of freshly prepared HS-ssDNA (probe) was hybridized with its complementary strand (target) in deoxygenated 10 mM Tris buffer at pH 7.4 containing 100 mM NaCl and 50 mM $MgCl_2$, by heating to 80 °C for 5 min followed by slow cooling to room temperature.

Prior to modification, the electrode arrays made from gold slides were cleaned with "piranha" solution at 90 °C for 8 min and then rinsed thoroughly with deionized water. Then each set (eight) of electrodes were modified simultaneously by spreading a drop of 20 μL of freshly prepared HS-ssDNA or HS-dsDNA in 10 mM Tris buffer (pH 7.4, also containing 100 mM NaCl and 50 mM $MgCl_2$). For FL characterization, the marker or target strand was modified with a fluorescent tag (Cy5) at the 3′- and 5′-end, respectively. The gold chips covered with DNA solution were stored in a sealed plastic box at 100% relative humidity at room temperature for 1~4 h. To prepare DNA SAMs on gold with varied surface densities, different concentrations (0.5~2.0 μM for ssDNA and 2.0~10 μM for dsDNA) were used in above steps while the incubation time was kept the same (1 h). After modification, the electrodes were incubated in 1 mM MCH solution for 1 h and thoroughly rinsed with 10 mM Tris buffer (pH 7.4) and water.

On-Chip Fluorescence and Electrochemical Characterization. The setup for on-chip potential control and fluorescence (FL) detection is shown in Scheme 2. All FL characterization was performed on a confocal laser-fluorescence scanner (Typhoon 9410, Amersham Biosystems). A thin PDMS plate (70 mm × 20 mm × 2.5 mm) with three small holes in the frame was inserted between the glass plate of the scanner and the gold chip, which can confine ~150 μL of electrolyte solution on the surface of the electrode array. All electrochemical experiments were carried out in this custom-made PDMS cell attached to the gold chip. The set of DNA-modified gold electrodes were used as working electrodes and a Ag|AgCl wire served as a reference electrode. A platinum wire inserted from the side was used as the counter electrode. A bipotentiostat (Autolab PGSTAT30, Eco Chemie BV, The Netherlands), which can individually control two working electrodes at the same time, was used to perform the measurements. Both cyclic voltammetric (CV) and chronocoulometric (CC) techniques were employed to measure the redox response of $[Ru(NH_3)_6]^{3+}$ cations bound electrostatically to the DNA SAMs, which allows the determination of the number of phosphate residues and thereby the surface density of the DNA strands.[10,40,41]

(39) Xia, Y.; Zhao, X. M.; Kim, E.; Whitesides, G. M. *Chem. Mater.* **1995**, *7*, 2332–2337.

(40) Yu, H.-Z.; Luo, C.-Y.; Sankar, C. G.; Sen, D. *Anal. Chem.* **2003**, *75*, 3902–3907.

Scheme 2. Electrochemical in Situ Fluorescence Imaging Setup[a]

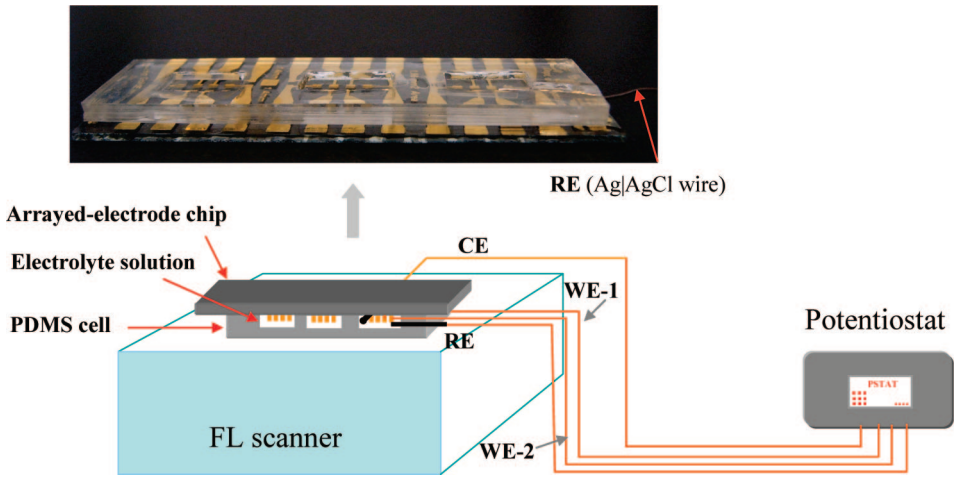

[a] The top inset is an optical image of the gold electrode array with a PDMS microcell attached to the chip surface.

All the CV and CC measurements were carried out at room temperature in 10 mM Tris buffer (pH 7.4) containing 5.0 μM or 50 μM $[Ru(NH_3)_6]Cl_3$, respectively. The electrodes were allowed to equilibrate with $[Ru(NH_3)_6]^{3+}$ for at least 15 min before starting the measurements. The solutions were deoxygenated and kept under an argon atmosphere throughout the experiments.

To study the electric field-assisted DNA hybridization, the electrode array modified with probe strands was immersed in 10 mM Tris buffer solution (pH 7.4) containing 50 or 100 mM NaCl and 0.1~0.5 μM target and biased at negative potential (−0.30 V), positive potential (+0.25 V), and open circuit potential (OCP) individually for different duration. Upon hybridization, the electrodes were washed with 10 mM Tris buffer for 5~10 min to remove the nonspecifically adsorbed DNA strands. Then the sample was characterized by FL scanning and CV (Scheme 2); the FL images and electrochemical data were analyzed by ImageQuant (Molecular Dynamics) and GPES (Autolab) software, respectively.

RESULTS AND DISCUSSION

Fabrication and Characterization of Gold Electrode Arrays. In the past, the inkjet printing technique, particularly using specially designed inkjet devices, has been successfully applied in the fabrication of polymer/metal microstructures, integrated circuits, microfluidic channels, and biomolecular arrays on various substrates.[42−49] Three technical issues must be addressed before commercial inkjet printers can be directly used as a drop-on-demand (DOD) tool to produce micropatterning or microdelivering tasks, i.e., ink compatibility, continuous ink filling, and substrate tolerance. The ink solution used for printing must be "mild" enough not to destroy the piezoelectric printer-head and must have an appropriate viscosity to be commensurate with the liquid flow requirement.[42] Cho et al. have recently demonstrated isopropanol is an ideal solvent for inkjet printing of *n*-alkanethiols.[38] Air bubble blocking is the major issue when filling the custom-made "ink" into the cartridges; this problem was solved in our case by adapting a continuous ink supply system (Figure 1). This setup also helps to configure the printer for large volume printing without the need for changing the cartridges. In this way, one refill of the ink tank is sufficient to print more than 1000 samples. We can easily print on papers or CD-Rs as the printer provides appropriate trays for loading them; however, on other substrates such as glass slides and metal foils it is not straightforward. We therefore designed a substrate holder: a regular CD-R with a cut-out slot that fits a standard microscope slide (2.5 cm × 7.5 cm). The entire arrangement can then be fed into the printer through its front-loading tray. The holder can be designed and made to accommodate substrates of different sizes and shapes. It should be pointed out that we also tested the upgraded versions (R220, R300, and R800) of Epson Stylus Photo printers, which produced equivalent or better printing results. Other manufactures (Canon and Primera, for example) also carry similar products, i.e., inexpensive office printers with a CD-print tray. The advances in the printer manufacture industry guarantees that the fabrication technique described here is not short-lived.

Resolution of the pattern and the quality of the surface are the two main criteria for making high-quality electrode arrays. The inkjet printing method reported here can offer a resolution of 50 μm (see Supporting Information), below which the designed patterns will become blurred and nonuniform. The 50 μm limit is not ideal according to the printer's specification (5750 × 1440 dpi, corresponding to 17.6 μm laterally), which is due to the spreading of thiol solutions on the hydrophilic gold substrates.[38] The quality of the final microstructures depends on the integrity of the thiolate SAMs formed on gold and the proper choice of etching conditions. A uniform SAM with closely packed structure and free of defects would be an ideal protection layer for the underneath gold film. To achieve this goal, not only the thiol concentration needs to be carefully chosen (~1.0 mM), the printing process should be also handled carefully. Printing the same pattern on the substrate

(41) Ge, B.; Huang, Y.-C.; Sen, D.; Yu, H.-Z. *J. Electroanal. Chem.* **2007**, *602*, 156–162.
(42) Calvert, P. *Chem. Mater.* **2001**, *13*, 3299–3305.
(43) Shimoda, T.; Morii, K.; Seki, S.; Kiguchi, H. *MRS Bull.* **2003**, *28*, 821–827.
(44) Gans, B. J.; Duineveld, P. C.; Schubert, U. S. *Adv. Mater.* **2004**, *16*, 203–213.
(45) Huang, D.; Liao, F.; Molesa, S.; Redinger, D.; Subramanian, V. *J. Electrochem. Soc.* **2003**, *150*, G412−G417.
(46) Yang, X.; Wang, Q.; Wang, K.; Tang, W.; Yao, J.; Li, H. *Langmuir* **2006**, *22*, 5654–5659.
(47) Watanabe, M. *Sens. Actuators, B* **2007**, *122*, 141–147.
(48) Goldmann, T.; Gonzalez, J. S. *J. Biochem. Biophys. Methods* **2000**, *42*, 105–110.
(49) Zaugg, F. G.; Wagner, P. *MRS Bull.* **2003**, *28*, 837–842.

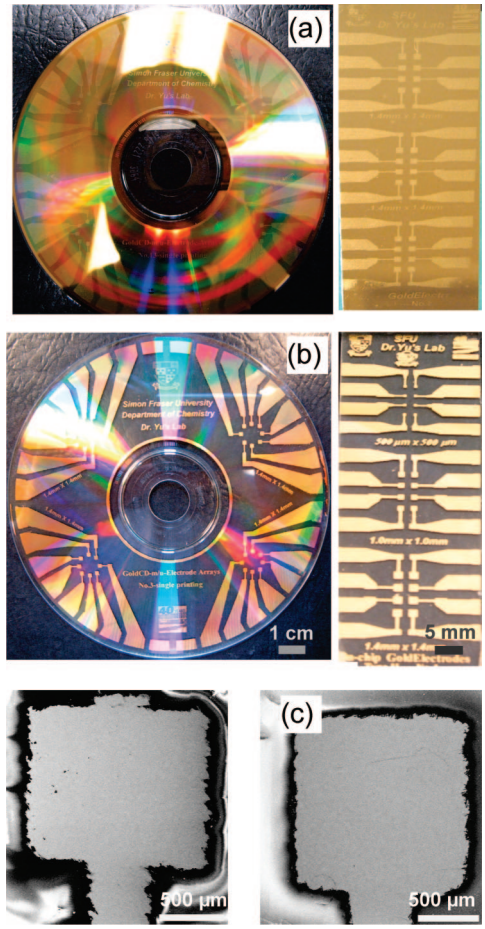

Figure 2. (a) Inkjet printed patterns (dried thiol solutions) on a gold CD-R and glass slide, (b) thus prepared electrode arrays after chemical etching, and (c) SEM images show individual electrodes fabricated from a gold CD-R (left) and glass slide (right), respectively.

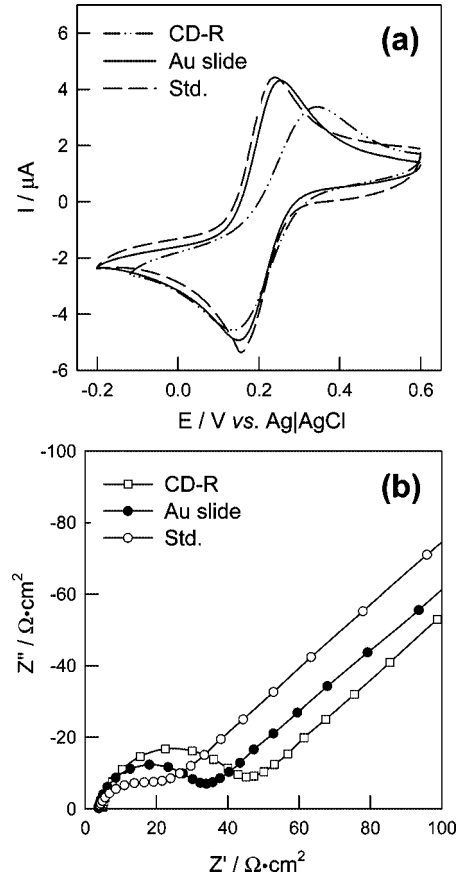

Figure 3. Electrochemical characterization of inkjet printed gold electrodes: (a) Cyclic voltammetric and (b) electrochemical impedance spectroscopic (EIS) responses of 1.0 mM $[Fe(CN)_6]^{3-}$/$[Fe(CN)_6]^{4-}$ in 0.1 M KCl on three different types of gold electrodes.

repeatedly seems to improve the quality of the SAMs. An example of the printed patterns (dried thiol solutions on gold substrates) is shown in Figure 2a, in which the designed structures were clear and the edges are well defined. It is also challenging to selectively etch a gold film with a thickness of 100 nm by using the typical wet-etching protocols. The etching condition must be optimized: besides the concentration and choice of etching reagents, the addition of "defect-healing" compounds and continuous stirring of the solution also helps. It was found that to saturate the etching solution with 1-octanol is beneficial to improve the resistance of the SAMs on the gold slides against chemical etching. 1-Octanol is lipophilic and has a high affinity for defects in *n*-alkanethiolate SAMs but not for the bare substrate.[50]

On the basis of the optimal printing and etching conditions established above, we can fabricate gold structures from either gold CD-Rs or gold slides with desired features. As shown in Figure 2b, arrayed electrodes with different sizes (from 300 μm to 1.4 mm) can be readily prepared. The individual electrode can be made as small as 100 μm × 100 μm with the currently printing/etching setup. Thus prepared electrodes have good conductivities without visible physical defects (Figure 2c). In particular, the edges of thus made electrodes are clearly defined (~20 μm as limited by the resolution of the inkjet printing process discussed above); the surface roughness of the gold film did not increase significantly either.[51] The electrical resistance of the electrodes prepared on gold CD-R and slides is typically 10~20 Ω and 3~5 Ω, respectively, which justifies their applications for practical electrochemical and solid-state electrical measurements. To further examine their performance, we compared the cyclic voltammetric (CV) and electrochemical impedance spectroscopic (EIS) responses of $[Fe(CN)_6]^{3-/4-}$ recorded on these electrodes (1.96 mm^2) and compared with a standard Au-disk electrode. As shown in Figure 3, for the three types of electrodes (CD-R, gold slides, and standard Au disk), the peak separations in the CV curves are 194, 94, and 80 mV while the radii of the impedance loops (i.e., the electron transfer resistance) in the EIS plots are 17.0, 12.0, and 8.0 Ω cm^2, respectively. Compared with the standard Au electrode, the one prepared from gold slides demonstrates excellent performance: almost identical CV curves with small peak separations and similar EIS plots with the comparable values of the electron transfer resistances. The one prepared from gold CD-Rs shows slightly deviated responses due to its inferior gold film (which is only ~50 nm thick and has an underneath dye layer);[51] however, it is still satisfactory for conventional electrochemical measurements.

(50) Geissler, M.; Schmid, H.; Bietsch, A.; Michel, B.; Delamarche, E. *Langmuir* **2002**, *18*, 2374–2377.

(51) Yu, H.-Z. *Anal. Chem.* **2001**, *73*, 4743–4747.

Potential Induced Conformational Switching of DNA SAMs on Gold. The inkjet printed electrode arrays are ideal platforms for parallel electrical analysis and manipulation of multiple analytes simultaneously on the same chip. As mentioned above, the electric field can be utilized to manipulate the conformation of DNA strands on the gold due to the electrostatic interactions between their negatively charged phosphate backbones and the electrode surface. The molecular orientation of the DNA strands can be repeatedly "switched" upon alternating the direction of the external electric field.[16−18] Therefore, for DNA molecules attached to the electrode and labeled with fluorescent tags, an "on/off" switching behavior is expected as a result of the conformational changes of DNA SAMs; this is due to the fact that the distance between the fluorophore and electrode surface dictates the extent of the fluorescence quenching.[13,14] To monitor this behavior clearly, it is necessary to keep the fluorophore at the end of DNA strands away from the gold surface by adjusting the DNA surface density[52] or applying an interfacial electric field.[16−20] We were able to achieve this goal by combining electrochemical modulation and FL imaging techniques together (Scheme 2); our inkjet printed electrode array on a standard glass slide provided a unique platform to study the conformational changes of DNA SAMs.

To study the conformational switching behavior of ssDNA SAMs, the oligomers (marker) that were Cy5-labeled at the 3′-ends and thiol-modified at the 5′-ends have been immobilized on the electrode surfaces. As shown in Figure 4a, the FL signal is directly related to the surface density of the DNA strands, i.e., the FL image becomes darker (higher FL intensity) with increased DNA surface density. However, if the DNA surface density reaches too high ($>10 \times 10^{12}$ molecule/cm^2), its signal will eventually saturate; if the density is too low ($<1 \times 10^{12}$ molecule/cm^2), no clear FL signal can be observed. Interestingly, even in the case of low surface density, we can substantially enhance the FL signal by applying a negative potential to the electrode. As shown in Figure 4b, about a 30% increase was observed at −0.3 V (vs Ag|AgCl); a ∼10% decrease in the FL signal was detected when shifting the electrode (WE-1) potential to 0.25 V from the OCP. Upon alternating the electrode potential from −0.3 to 0.25 V repeatedly, we can observe a reproducible "on/off" behavior of the observed FL signal. More importantly, we were able to monitor such a FL switching behavior on two independent electrodes (WE-1 and WE-2) simultaneously by using a dual-channel potentiostat that can control two working electrodes independently at the same time. During this electrical manipulation process, the electrode potential needs to be chosen carefully. It has been confirmed that the potential range from −0.4 to +0.4 V with respect to the point of zero charge (PZC, 0.1∼0.2 V vs Ag|AgCl) is "safe" (no reductive or oxidative desorption of the thiolate DNA monolayers is expected) for electrochemically switching the molecular orientation of the DNA SAMs on gold.[16−18,53] For the modulation amplitude (the change of the FL intensities upon shifting the electrode potential), DNA surface density was also found to play an important role. As shown in Figure 4c, when the surface density decreased from $(18 \pm 2) \times 10^{12}$ to $(2.8 \pm 0.5) \times 10^{12}$ molecules/cm^2, the modulation amplitude increased from 2% to 28%. Steric interaction among DNA strands tethered to the chip surface to prevent their reorientation induced by the electrical field; therefore, the variation of the observed FL intensities upon shifting the potential was not substantial.[16,52]

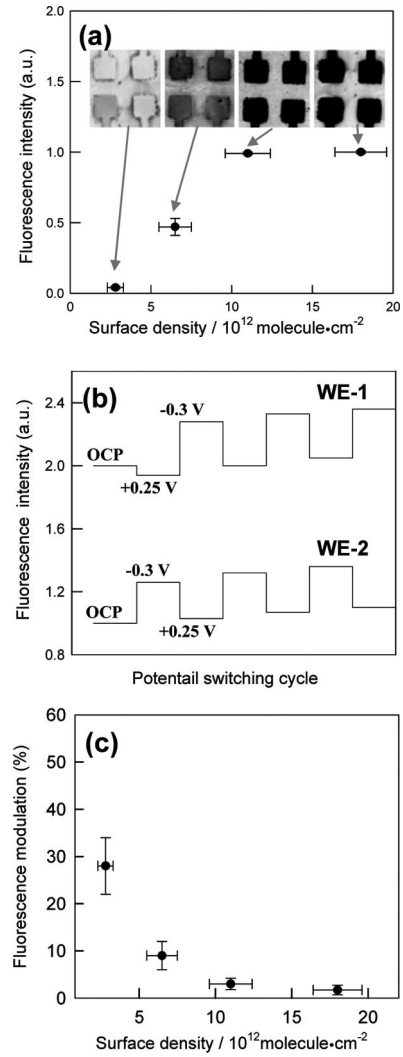

Figure 4. (a) The correlation between the observed fluorescence (FL) signal from Cy5-labeled ssDNA SAMs on gold and the DNA surface density. The insets are the FL images of gold electrode arrays modified with Cy5-labeled ssDNA of varied surface densities, (b) dependence of the FL intensity on the electrode potential observed at two independent working electrodes (WE-1 and WE-2); the absolute intensity values for the two electrodes were offset for clarity purpose, and (c) the correlation between the surface density of ssDNA SAMs and the observed FL modulation amplitude.

To examine the conformational switching behavior of dsDNA SAMs, the chip with arrayed electrodes was immersed in thiol-terminated dsDNA solution (thiolate probe hybridized with fluorescently labeled target in solution first). As shown in Figure 5a, the FL signal from the dsDNA monolayer is also dependent on the surface density; however, the FL intensity is much higher than that of an ssDNA monolayer. This is attributed to the fact that the relatively "stiffer" backbone and stronger intermolecular interaction of dsDNA lead to the fluorescent tags further away from the gold surface compared to the case of ssDNA. Besides, the more rigid structure of dsDNA offers a more distinct FL "switching" behavior upon applying alternate electric fields. As

(52) Rant, U.; Arinaga, K.; Fujita, S.; Yokoyama, N.; Abstreiter, G.; Tornow, M. *Langmuir* **2004**, *20*, 10086–10092.
(53) Dong, L. Q.; Zhou, J. Z.; Wu, L. L.; Dong, P.; Lin, Z. H. *Chem. Phys. Lett.* **2002**, *353*, 458–465.

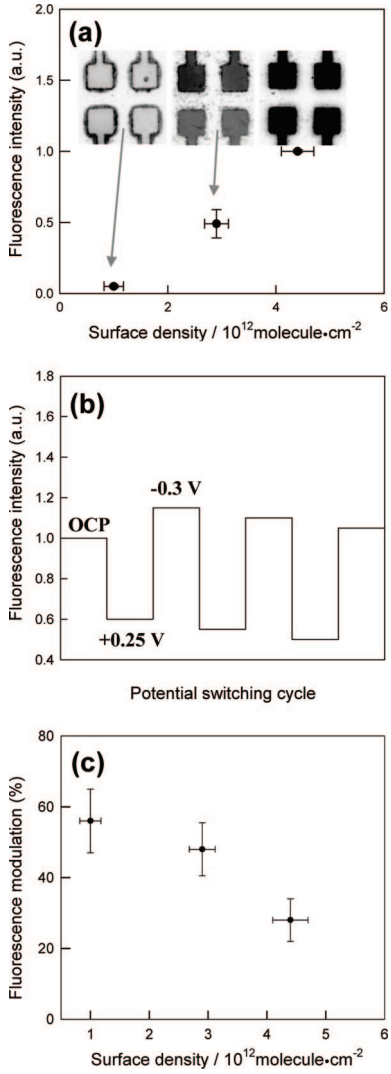

Figure 5. (a) The correlation between the observed FL signal from Cy5-labeled dsDNA monolayers on gold and the surface density. The insets are the FL images of gold electrode arrays modified with Cy5-labeled dsDNA SAMs of varied surface densities, (b) dependence of FL intensity on the applied electrode potential, and (c) the correlation between surface density of dsDNA SAMs and the observed FL modulation amplitude.

shown in Figure 5b, above 50% enhancement in the FL signal was detected upon shifting its potential from +0.25 to −0.3 V (vs Ag|AgCl). The surface density of dsDNA SAMs was also found to affect the structural manipulation under electric fields. As the surface density decreasing from $(4.4 \pm 0.3) \times 10^{12}$ to $(1.0 \pm 0.2) \times 10^{12}$ molecules/cm^2, the modulation amplitude was increased from 28% to 56% (as shown in Figure 5c). The upper limit is about twice as large as that of ssDNA SAMs with similar surface density. To understand the difference, we need to consider the respective molecular conformation in these two different cases: the end-tethered ssDNA strands extend from the surface like "ropes" with coiled top parts; while the dsDNA molecules may be represented by straight "rods". Generally, the strong interfacial electric field only exists in a range proximal to the electrode surface (typically a few nanometers) due to the screening effect from the electrolyte.[16,17] Therefore only the lower portion can be affected by the electric field for a surface-tethered 30 mer DNA strand (~10 nm for the total length). The fluorescent tags at the top ends for dsDNA thus can be manipulated to be further away from the gold surface upon shifting the polarity of the electric field, which results in a more significant variation in the FL intensities.[16] Rant et al. have proposed a plausible "charge-rod" model to semiquantitatively simulate the dependence of the FL intensity on the molecular orientation of DNA monolayers (i.e., on the distance between the FL tags and electrode surface) on gold.[17]

Electric Field-Assisted DNA On-Chip Hybridization. The success of using inkjet printed electrode arrays for the electrical modulation of DNA SAMs provides us an opportunity to manipulate the on-chip DNA hybridization process (i.e., to explore the effect of interfacial electric fields). As mentioned above, there are significant electrostatic interactions between the charged DNA strands and the electrode surface; therefore, the interfacial electric fields not only modulate the molecular orientation of surface-tethered DNA strands but also influence the mobility of DNA strands in the solution (nearby the electrode). With dependence on its surface charging state, the electrode may attract or repel solution-defused DNA molecules and thus facilitate or inhibit the on-chip DNA hybridization process.[27,28] To investigate this phenomenon, the DNA probe-modified electrodes were immersed in a Cy5-labeled target solution while applying potentials for various durations. All the hybridization assays and electrochemical characterizations were carried out in the microcell made of a PDMS plate as shown in Scheme 2. After hybridization, the chips were washed and then characterized by FL scanning and CV measurements, respectively.

We were able to control two working electrodes simultaneously by using the dual-channel potentiostat, which allowed us to examine DNA hybridization experiments done at three different potential settings (including OCP). Figure 6a shows the FL images obtained on the electrodes that were under different potentials: the right two were at −0.3 (top) and 0.25 V (bottom), respectively; the left two were both at OCP (no external potential exerted). It was found that the hybridization signals on these electrodes followed a similar trend, i.e., increased rapidly in the first 100 s and then reached a plateau after about 300 s. However, the FL signal obtained under positive potential was 1.2 and 1.8 times higher than that of OCP or negative potentials, respectively (Figure 6b). The nonuniformity exhibited in these FL images (compared with those in Figures 4 and 5) is probably attributed to the different hybridization efficiencies across the surface, which highly depends on both the local packing density and molecular orientation of the DNA probe strands on the surface. We also confirmed the hybridization results by carrying out CV measurements in the presence of 5 μM $[Ru(NH_3)_6]^{3+}$. As shown in Figure 7, for the electrode under the positive potential, its peak current increased from 28% to 57% with the hybridization time extended from 100 to 600 s. The hybridization signal (integrated charge) in this case is about 1.4 and 1.9 times higher than those obtained under OCP and the negative potential, respectively. Unlike the electric field-assisted hybridization experiments reported before,[21,26,28] the combination of the fabrication of electrode arrays and in situ FL monitoring of DNA hybridization offers unique opportunities for us to further understand the structure and behavior of DNA molecules on a chip.

It should be noted that the surface density of DNA probes, the salt concentration, and the target concentration directly affect

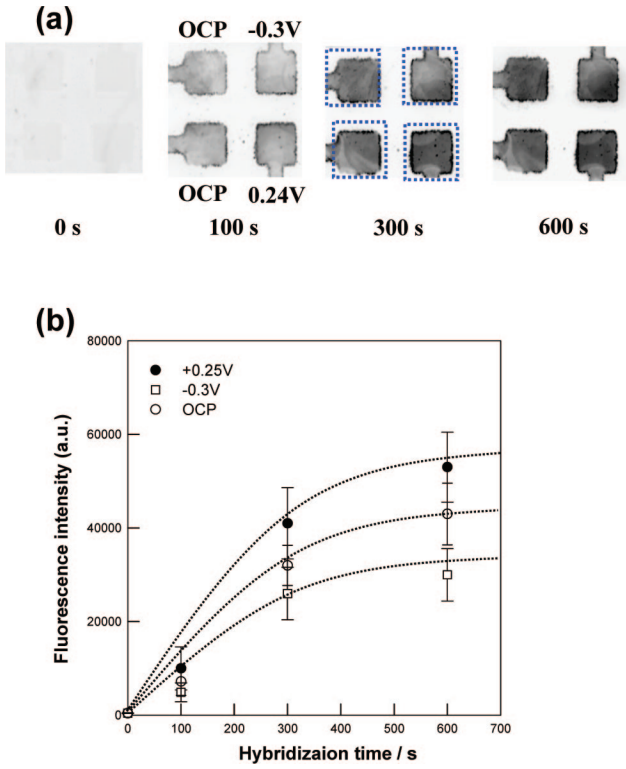

Figure 6. In situ FL monitoring of the DNA on-chip hybridization process under electrochemical potential control: (a) FL images recorded at different hybridization duration showing the comparison among different potential settings; and (b) the correlation between the observed FL intensity (target signal) and the hybridization time.

the hybridization dynamics.[16,17,23,52] Among these factors, the effect from salt concentrations is complex: the presence of metal cations helps DNA hybridization by decreasing the repulsive forces between probe and target strands; however, they may also screen the effect from interfacial electric field.[16,17] It was found that 10 mM Tris buffer containing 50 or 100 mM NaCl is a suitable solution for conducting DNA hybridization experiments. Another concern in the present study is the effect of the molecular conformation of DNA probes on the hybridization efficiency.[53] As mentioned above, interfacial electric fields not only affect the transport of DNA in solution but also modulate the molecular orientation of DNA strands tethered to the metal surface. Thus, the alternated electric field with appropriate frequency and amplitude is anticipated to have the possibility of taking care of these two factors simultaneously.

CONCLUSIONS

We have developed a simple and cost-effective fabrication protocol for making gold electrode arrays; standard office inkjet printers can be adapted to deliver alkanethiol solutions on gold to form resist layers, and a typical wet-chemical etching method can be used to release the patterns. The electrode arrays can be made with desired size and shape and showed ideal electrochemical performances when tested with standard redox reactions (both cyclic voltammetric and impedance spectroscopic studies of $[Fe(CN)_6]^{3-/4-}$). In addition, they can be used to examine the electrical modulation of the molecular orientation of thiolate DNA

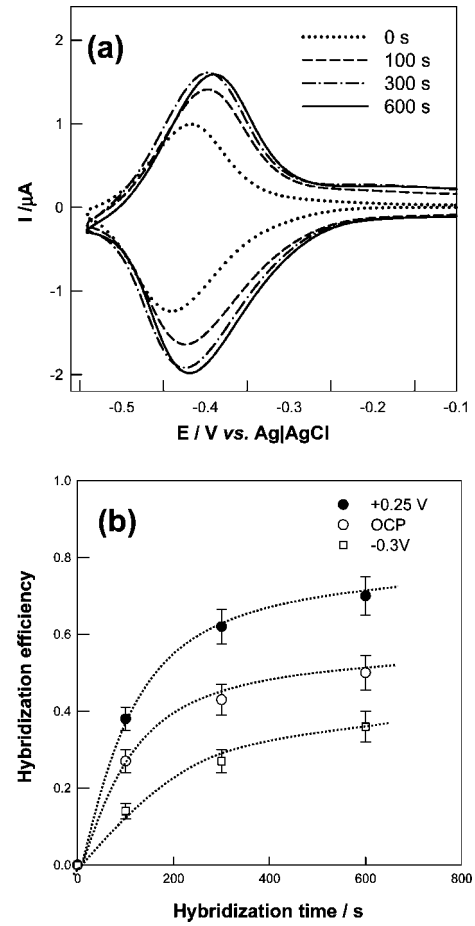

Figure 7. Electrochemical monitoring of the on-chip DNA hybridization process: (a) CVs of 5.0 μM $[Ru(NH_3)_6]^{3+}$ on the electrode under positive potential control recorded at different hybridization time and (b) the correlation between the integrated charges (hybridization signal) and the hybridization time.

SAMs formed upon. It is feasible to carry out fluorescence scanning simultaneously while varying the electrode potential, which provides the opportunity to study the on-chip hybridization process under potential control. We confirmed that the interfacial electric field is able to either facilitate or inhibit DNA on-chip hybridization, which is dictated by the polarity of the applied electrode potential.

ACKNOWLEDGMENT

We acknowledge the help of Mr. Hanjin Cho and Mr. Lin Wang on the experiments. This research is supported by the funds from Natural Science and Engineering Research Council of Canada (NSERC).

SUPPORTING INFORMATION AVAILABLE

Experimental details for the preparation of gold electrode arrays and their structural characterizations. This material is available free of charge via the Internet at http://pubs.acs.org.

Received for review July 10, 2008. Accepted September 27, 2008.

AC801420H